

## Article

# Enhanced Photocatalytic Activity of ZnO-Graphene Oxide Nanocomposite by Electron Scavenging

Syed Nabeel Ahmed and Waseem Haider \*

School of Engineering &amp; Technology, Central Michigan University, Mt. Pleasant, MI 48859, USA; ahmed1sn@cmich.edu

\* Correspondence: haide1w@cmich.edu

**Abstract:** Advances in nanotechnology have opened new doors to overcome the problems related to contaminated water by introducing photocatalytic nanomaterials. These materials can effectively degrade toxic contaminants, such as dyes and other organic pollutants, into harmless by-products such as carbon dioxide and water. Consequently, these photocatalytic nanomaterials have the potential to provide low-cost and environment-friendly alternatives to conventional water and wastewater treatment techniques. In this study, a nanocomposite of zinc oxide and graphene oxide was developed and evaluated for photocatalysis. This nanocomposite was characterized by XRD, FTIR, FESEM, Diffuse Reflectance Spectroscopy (DRS), TEM and UV-Vis spectrophotometer. The photocatalytic behavior of the nanocomposite was studied through the degradation of methyl orange under ultraviolet light. It is reported that the weight ratios of zinc oxide and graphene oxide do not considerably affect the photocatalytic performance, which gives this process more compositional flexibility. Moreover, hydrogen peroxide was used as an electron scavenger to increase the time-efficiency of the process. The photodegradation rate can be significantly improved (up to 24 times) with the addition of hydrogen peroxide, which increases the number of trapped electrons and generates more oxidizing species, consequently increasing the reaction rate.



**Citation:** Ahmed, S.N.; Haider, W. Enhanced Photocatalytic Activity of ZnO-Graphene Oxide Nanocomposite by Electron Scavenging. *Catalysts* **2021**, *11*, 187. <https://doi.org/10.3390/catal11020187>

Received: 15 October 2020

Accepted: 20 January 2021

Published: 31 January 2021

**Publisher's Note:** MDPI stays neutral with regard to jurisdictional claims in published maps and institutional affiliations.



**Copyright:** © 2021 by the authors. Licensee MDPI, Basel, Switzerland. This article is an open access article distributed under the terms and conditions of the Creative Commons Attribution (CC BY) license (<https://creativecommons.org/licenses/by/4.0/>).

**Keywords:** nanocomposite; photocatalysis; wastewater treatment

## 1. Introduction

Unavailability of clean water is one of the fastest growing problems in today's world. It is estimated that about 3.6 billion people live in areas that are potentially water-scarce at least one month per year [1]. Due to a 1% increase in the global water demand every year [1], efforts are being made to find low-cost [2] and environmentally friendly [3] ways of reclaiming wastewater. These efforts have introduced heterogeneous photocatalysis as a potential alternative to conventional wastewater treatment techniques [4–6]. However, in real world applications, photocatalytic processes still face challenges due to higher reaction times for batch-type processes, and lower efficiencies and recyclability for continuous type processes. Therefore, efforts are being made to improve the efficiency and to reduce the reaction time of the process. These efforts include better photocatalytic reactor design, modification of photocatalysts by doping and heterojunction, and the use of electron scavengers [6].

Among the most widely studied photocatalysts, zinc oxide is a wide band-gap photocatalytic semiconductor which has gained significant attention during the past years, particularly due to the fact that some researchers have reported ZnO demonstrating a better photocatalytic efficiency than the most widely studied TiO<sub>2</sub> [7,8]. The wide bandgap of ZnO not only makes it highly sensitive to ultra-violet light, but also causes the emission of the blue as well as green light post-irradiation. This emission corresponds to the exciton and defect recombination, which is extremely helpful for photocatalytic applications [9]. However, due to the wide bandgap of ZnO, it is difficult to photoexcite electrons under visible light irradiation [10].

It has been reported that hybridizing ZnO with graphene oxide (GO) enhances its photocatalytic activity by providing spatial separation of the photogenerated electrons and holes and preventing electron-hole recombination. Additionally, the large specific surface area of graphene increases the reaction rate by providing more active sites for adsorption. Furthermore, the lower potential of graphene/graphene<sup>-</sup> enables the rapid electron migration from the semiconductor to the graphene [11]. Consequently, many researchers have demonstrated excellent tendency of graphene based ZnO nanocomposites for the degradation of harmful organic compounds, which include methylene blue [12,13], rhodamine B [14], and deoxynivalenol [15]. Moreover, ZnO based nanocomposites have also been reported to have excellent tendency towards the degradation of bacteria [16,17] as well as toxic metal ions [18,19]. Despite all these advantages and decades of research, photocatalysis is still limited to the laboratories and still not feasible for commercial scale, particularly due to very high reaction times. This study aims to solve this issue by accelerating the reaction rate through electron scavengers.

In this study, we have developed a series of ZnO-GO nanocomposites by decorating ZnO nano-powder on graphene oxide sheets in four different ratios of GO:ZnO by weight. The photocatalytic behavior of the resulting nanocomposites has been assessed by studying the degradation of methyl orange in aqueous medium, which is one of the most hazardous chemicals in industrial wastewater. One of the best ways to enhance the photodegradation rate is adding an electron-hole scavenger to increase the number of trapped electrons [20]. Therefore, in this study, we have used hydrogen peroxide (H<sub>2</sub>O<sub>2</sub>) as an electron scavenger to increase the time-efficiency of the process.

## 2. Results and Discussion

Figure 1a demonstrates the TEM images of the graphene oxide sheets, with the inset showing the selected area diffraction pattern of graphene oxide. The morphology of as-synthesized GO exhibited the stacking pattern of graphene layers. The FESEM image of the prepared nanocomposite (sample 1:10) is shown in Figure 1b. Figure 1c,d illustrates the TEM images of ZnO-GO nanocomposite. It can be seen that ZnO nanoparticles were exhibiting irregular powder-like morphology and were attached to GO sheets. Some ZnO particles were agglomerated on the GO sheets.

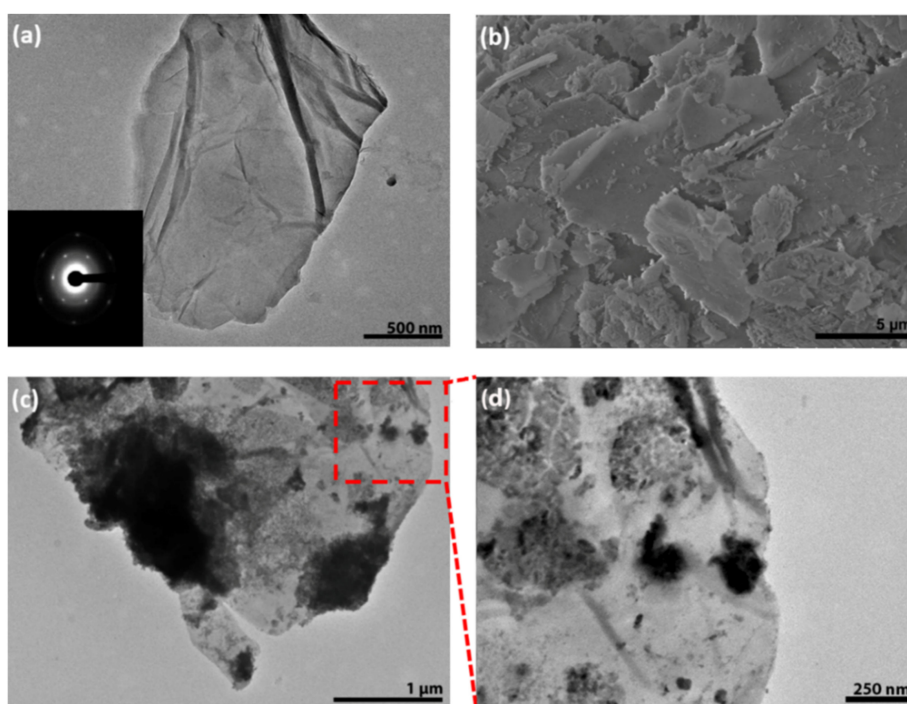


**Figure 1.** (a) TEM image of undecorated graphene oxide (GO), inset shows the diffraction pattern, (b) FESEM image of graphene oxide decorated with ZnO nano-powder (1:10) (c) TEM image of graphene oxide decorated with ZnO nanopowder (1:15) and (d) High magnification TEM view of GO-ZnO nanocomposite.

For studying the composition and crystallographic planes, the prepared nanocomposites have been characterized by XRD and infrared spectroscopy. Figure 2a shows the XRD plot of ZnO-GO nanocomposites with all four weight ratios, indicating the crystallographic planes of ZnO. The peaks at  $31.7^\circ$ ,  $34.4^\circ$ ,  $36.2^\circ$ ,  $47.5^\circ$ ,  $56.5^\circ$ ,  $63.0^\circ$ ,  $68.0^\circ$ ,  $69.0^\circ$ ,  $72.1^\circ$  and  $76.7^\circ$  can be indexed to the (100), (002), (101), (102), (110), (103), (112), (201), (004) and (202) planes of Wurtzite ZnO, respectively.

To further confirm the interaction between ZnO and GO, FTIR spectrum has been recorded. Figure 2b demonstrates the infrared spectra of pure GO, commercial ZnO powder, as well as one of the prepared GO-ZnO nanocomposites (1:10). The bending and stretching of zinc oxygen double bonds generate an absorption peak at a very low wavenumber which even goes below  $400\text{ cm}^{-1}$ , whereas the hydroxyl group bending and stretching peaks can be seen in the GO and ZnO-GO samples at  $1572\text{ cm}^{-1}$  and  $3350\text{ cm}^{-1}$ , respectively. The C-O stretching vibration can be observed at  $1072\text{ cm}^{-1}$ , whereas the noise at around  $2000\text{ cm}^{-1}$  in all three of the infrared spectra is due to the diamond tip of the equipment that comes in contact with the sample.

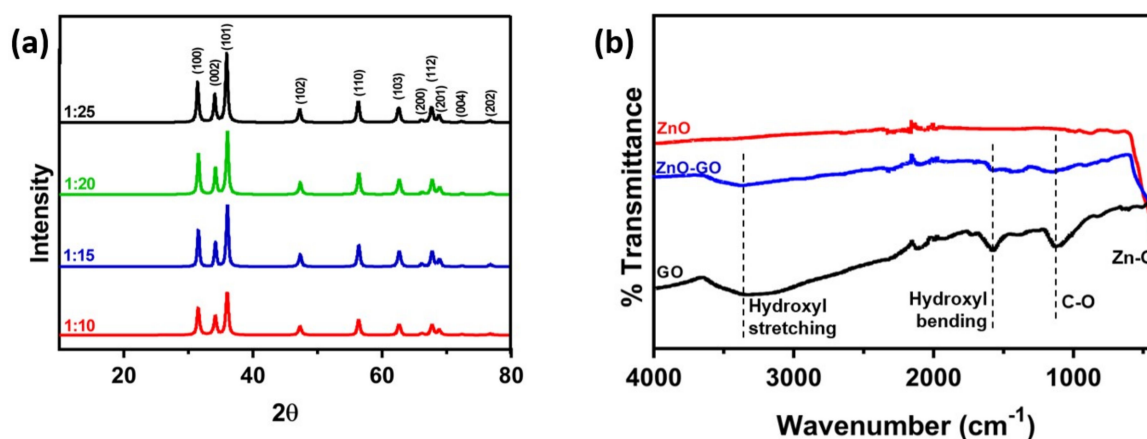


**Figure 2.** (a) XRD of the ZnO-GO nanocomposites with different ratios showing the crystallographic planes of ZnO and (b) FTIR of commercial ZnO powder, pure GO and the ZnO-GO nanocomposite (1:10).

The photocatalytic performance of the nanocomposites is illustrated in Figure 3a–d. All four samples show a complete degradation of dye after 9 h of irradiation. It should be noted that the weight ratios of GO and ZnO do not have a significant effect on the photocatalytic efficiency, since all four samples show almost the same degradation rate. Upon irradiation, the electrons in the valence band of ZnO are first photoexcited, and transferred into the conduction band. These transferred electrons produce negative and positive charge carriers called electrons and holes, respectively. The work function of ZnO (5.2–5.3 eV) is different from that of GO (4.5 eV), so photoexcited electrons transfer readily from ZnO to GO [21,22]. Subsequently,  $\bullet\text{OOH}$  radicals and the trapped electrons combine to produce  $\text{H}_2\text{O}_2$ , finally forming  $\bullet\text{OH}$  radicals. These radicals are mainly responsible for the degradation of methyl orange.

In order to enhance the photocatalytic performance,  $\text{H}_2\text{O}_2$  (0.4 mol/L) was added in the reaction solution. Figure 4a–d indicates that the addition of  $\text{H}_2\text{O}_2$  has significantly enhanced the photocatalytic performance by almost 24 times. This can be explained by the ability of  $\text{H}_2\text{O}_2$  to prevent electron-hole recombination by adding electron acceptors to the reaction, which increases the number of trapped electrons. Another way that explains the significant enhancement in the photocatalytic activity is that  $\text{H}_2\text{O}_2$  generates more  $\bullet\text{OH}$  radicals and other oxidizing species. Additionally, problems caused by  $\text{O}_2$  starvation are also overcome and the oxidation rate of intermediate compounds is also increased by the addition of  $\text{H}_2\text{O}_2$  [23]. All these factors, which include the added electrons,  $\bullet\text{OH}$  radicals and the availability of oxygen, act synergistically and explain the decrease in the photocatalytic degradation time to almost 4% of the original time, after the addition of

0.4 mol/L of hydrogen peroxide, as shown in Figure 4a–d. It should be highlighted that the concentration of hydrogen peroxide should be carefully controlled since it can render the water toxic at higher concentrations. However, 0.4 mol/L of hydrogen peroxide is much lower than its concentration typically used in households (3–10%). Table 1 summarizes the photocatalytic performance of pure ZnO and ZnO-GO nanocomposites from recent studies in various heterojunctions. It can be observed that the ZnO-rGO photocatalysts show a significant improvement in photocatalytic performance compared to past studies.

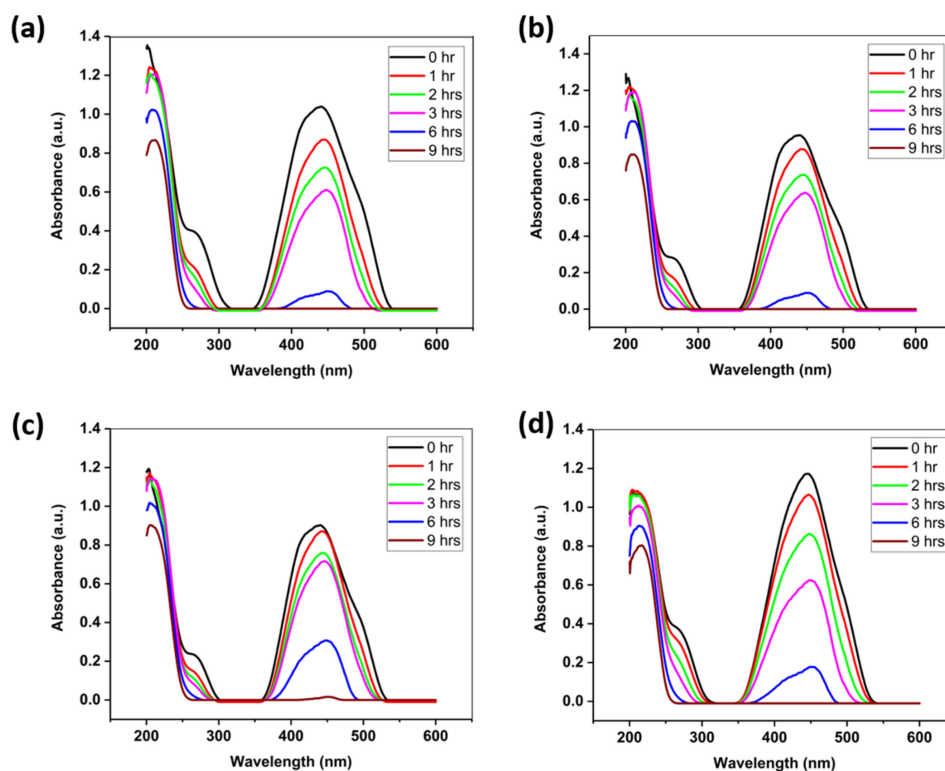


**Figure 3.** Photocatalytic activity of the prepared nanocomposites of ZnO-GO with (a) 1:10 ratio (b) 1:15 ratio (c) 1:20 ratio and (d) 1:25 ratio.

**Table 1.** Photocatalytic performance of ZnO-GO based nanocomposites.

Composition	Light Source	Pollutant	Experimental Conditions	Photocatalytic Efficiency (Pollutant Removal)	Reference
ZnO	100 W UV	Methylene Blue (15g/L)	CL = 1.25 g/L $t_r$ = 80 min	76%	[24]
ZnO-rGO	Sunlight	Methylene Blue (15g/L)	CL = 1.25 g/L $t_r$ = 150 min	97%	[24]
ZnO-rGO	300 W UV	Methylene Blue (0.01g/L)	CL = 0.5 g/L $t_r$ = 120 min ID = 10 cm	99%	[25]
ZnO-graphene	UV (365 nm)	Deoxynivalenol (15 mg/L)	CL = 0.5 mg/L $t_r$ = 30 min	~99%	[15]
ZnO-GO	300 W visible	Methylene Blue (0.03126 mM/L)	CL = 0.1 g/L $t_r$ = 120 min ID = 10 cm	12%	[10]
ZnO-GO	250 W UV	Methylene Blue (960 mg/L)	CL = 0.25 g/L $t_r$ = 450 min	~75%	[13]
Au-ZnO-rGO	UV and Visible	Rhodamine B (94%)	CL = IM $t_r$ = 180 min ID = 1 cm	94%	[14]
ZnO-rGO	20 W UV	Methylene Blue (25 mg/L)	CL = 0.1 g/L $t_r$ = 30 min ID = 10 cm	~86%	[26]

$t_r$  = Irradiation time. CL = Catalyst Loading. ID = Irradiation distance.

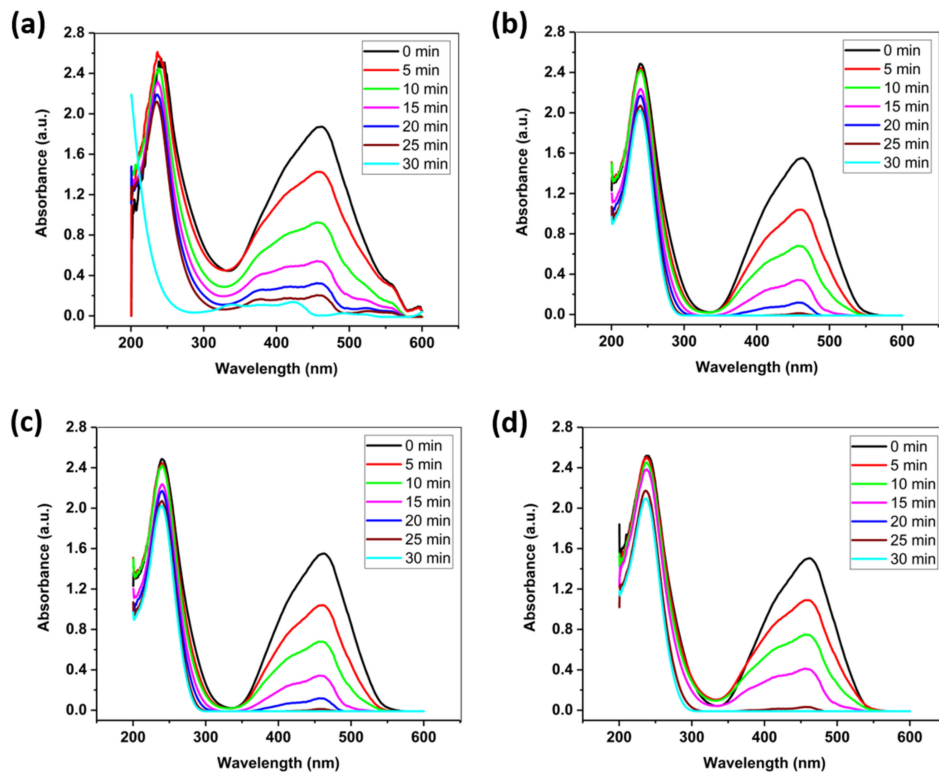


**Figure 4.** Photocatalytic activity of the prepared nanocomposites of ZnO-GO with (a) 1:10 ratio (b) 1:15 ratio (c) 1:20 ratio and (d) 1:25 ratio after adding  $\text{H}_2\text{O}_2$ .

For studying the effect of graphene hybridization on the bandgap of the nanocomposite, UV-Vis Diffuse Reflectance Spectroscopy (DRS) has been performed (Figure 5a). Figure 5b shows the Tauc plots obtained from UV-Vis DRS and from these plots, the bandgap of the nanocomposites has been found to be 3.3 eV. These results indicate that the bandgap of the nanocomposite is independent of the weight percentage of GO in the GO-ZnO nanocomposites, thereby confirming their somewhat similar photocatalytic behavior. The presence of GO provides a higher surface area and the addition of hydrogen peroxide significantly improved the photodegradation reaction rate (upto 24 times), thus improving the photocatalytic efficiency or pollutant removal. Moreover, the addition of  $\text{H}_2\text{O}_2$  significantly reduces the reaction time to about 4% of the original time by increasing the number of trapped electrons and generating more oxidizing species. As far as the durability is concerned, the photocatalysts have to be separated from the solution for reuse, which adds up to the cost and time of the process. Therefore, in terms of durability, a batch type photocatalytic process still needs more improvement than its less efficient continuous type counterpart.

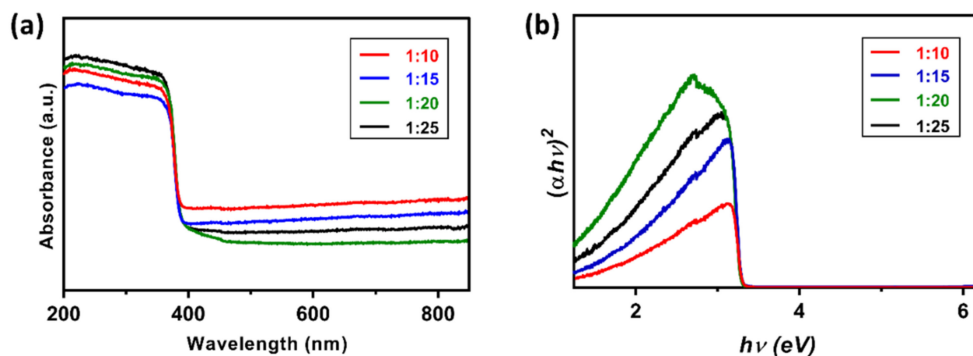


**Figure 5.** (a) UV-Vis Diffuse Reflectance Spectroscopy (DRS) spectra of ZnO-GO nanocomposites with different weight percentages, and (b) Tauc plot obtained from DRS.

### 3. Experimental Methods

#### 3.1. Preparation of Graphene Oxide

For the preparation of graphene oxide, improved Hummers' method has been employed [20]. Briefly, concentrated sulfuric acid (69 mL) was first added to a mixture of 2 g of graphite flakes and 1.5 g of sodium nitrate and the mixture was cooled using the water circulation bath to 5 °C. A total of 9 g of potassium permanganate was then added slowly in portions to keep the reaction mixture temperature below 20 °C. The temperature was then raised to 35 °C and the solution was magnetically stirred for 7 h. A total of 9 g of potassium permanganate was then added again in one portion, and the reaction mixture was stirred continuously for 12 h at the same temperature. The reaction mixture was then cooled to room temperature, followed by the addition of cold Deionized (DI) water (2–5 °C) and 3 mL of 30% H<sub>2</sub>O<sub>2</sub>. The mixture was then purified using the same protocol of filtering/centrifugation as before, decanting with multiple washes by 30% HCl and ethanol. The product was then dried under vacuum overnight at 40 °C [27].

#### 3.2. Decoration of ZnO Nanopowder

For the decoration of ZnO powder, 0.02 moles of Zn(NO<sub>3</sub>)<sub>2</sub> were dissolved in 100 mL of DI water at 5 °C. Separately, graphene oxide was dispersed in 200 mL of DI water and ultrasonicated for 60 min, and then mixed with the Zn(NO<sub>3</sub>)<sub>2</sub> solution under vigorous stirring. The pH was adjusted to 8 by adding 1 M KOH dropwise, and the solution was magnetically stirred for 12 h. Finally, the product was centrifuged for 12 h in vacuum and dried at 60 °C, and then heat treated at 200 °C in air for two hours. Using this method, the GO-ZnO nanocomposites were prepared in four different weight ratios, which are 1:10, 1:15, 1:20 and 1:25. The reason for selecting this range of composition is that at higher percentages of graphene composites, the photocatalytic efficiency decreases due to the shielding effect caused by graphene [9], whereas at narrower percentages, the effect of graphene hybridization is negligible. All the photocatalytic experiments were performed at room temperature.

### 4. Characterization

X-ray diffraction (XRD) analysis for the prepared nanocomposites was performed in the range of  $2\theta = 10\text{--}90^\circ$  at the rate of  $1^\circ/\text{min}$ , by using Rigaku Miniflex II X-ray diffractometer (Rigaku, Tokyo, Japan). The composition/functional property of the nanocomposites was studied with FTIR spectroscopy at room temperature in an acquired range of  $500\text{--}4000\text{ cm}^{-1}$ . For the FTIR, the Thermo scientific Nicolet iS50 FT-IR (Thermo Scientific, Waltham, MA USA) was used. The structure and morphology of the nanocomposites were studied with Transmission Electron Microscopy (TEM), Selected Area Electron Diffraction (SAED) and Field Emission Scanning Electron Microscopy (FESEM). TEM and SAED were carried out using Hitachi Model HT7700 (Hitachi, Tokyo, Japan) using high resolution mode at 120kV.

#### Photocatalytic Studies

For the photocatalytic studies, 3 mL of methyl orange solution (20 mg/L) was mixed with 3 mg of the GO-ZnO nanocomposite. Prior to irradiation, the sample was kept in the dark for 60 min for the adsorption-desorption equilibrium, and then irradiated with ultra-violet (UV) light of wavelength 253 nm (UVC). The measurements were taken through an Ocean Optics UV-Vis spectrophotometer (Ocean Optics, Orlando, FL, USA), at different time intervals (0, 1, 2, 3, 9 h). The photocatalytic studies have also been performed in the presence of 0.4 mol/L of hydrogen peroxide. For band-gap measurements, UV-Vis Diffuse Reflectance Spectroscopy (DRS) was performed and the band gap energies were calculated from a plot  $(\alpha h\nu)^2$  versus photo-energy ( $h\nu$ ) using the Kubelka–Munk function, which shows the relationship between the band gap and the absorption coefficient.

## 5. Conclusions

In this study, GO-ZnO nanocomposites have been prepared with four different weight ratios, which are 1:10, 1:15, 1:20 and 1:25, respectively. These nanocomposites have been characterized by using TEM, SAED, FESEM, XRD and FTIR. The photocatalytic behavior of these nanocomposites has been studied with and without H<sub>2</sub>O<sub>2</sub> as an electron scavenger. It has been concluded that varying the compositions does not show a considerable difference in the photocatalytic activity of the nanocomposites, which has been further confirmed by their bandgaps (3.3 eV). Therefore, such nanocomposites can be prepared and utilized on large scales, without paying attention to compositional variations. Consequently, problems related to localized heterogeneities and segregations can also be avoided. Furthermore, the addition of H<sub>2</sub>O<sub>2</sub> significantly reduces the reaction time to about 4% of the original time by increasing the number of trapped electrons and generating more oxidizing species. Hence, H<sub>2</sub>O<sub>2</sub> as an electron scavenger can be very useful in actual water treatment applications and can significantly improve the time efficiency of the process.

**Author Contributions:** Conceptualization, S.N.A. and W.H.; methodology, S.N.A.; writing—original draft preparation, S.N.A.; writing—review and editing, W.H.; supervision, W.H.; project administration, W.H. All authors have read and agreed to the published version of the manuscript.

**Funding:** This research received no external funding.

**Data Availability Statement:** All the data generated during this study is reported in this article.

**Conflicts of Interest:** The authors declare no conflict of interest.

## References

1. United Nations. The United Nations World Water Development Report 2018: Nature-Based Solutions for Water. 2018. Available online: <http://unesdoc.unesco.org/images/0026/002614/261424e.pdf> (accessed on 1 January 2020).
2. Bouazizi, A.; Breida, M.; Achiou, B.; Ouammou, M.; Calvo, J.I.; Aaddane, A.; Younsi, S.A. Removal of dyes by a new nano-TiO<sub>2</sub> ultrafiltration membrane deposited on low-cost support prepared from natural Moroccan bentonite. *Appl. Clay Sci.* **2017**, *149*, 127–135. [[CrossRef](#)]
3. Friedmann, D.; Hakki, A.; Kim, H.; Choi, W.; Bahnemann, D. Heterogeneous photocatalytic organic synthesis: State-of-the-art and future perspectives. *Green Chem.* **2016**, *18*, 5391–5411. [[CrossRef](#)]
4. Ayekoe, C.Y.P.; Robert, D.; Lancine, D.G. Combination of coagulation-flocculation and heterogeneous photocatalysis for improving the removal of humic substances in real treated water from Agbo River (Ivory-Coast). *Catal. Today* **2017**, *281*, 2–13. [[CrossRef](#)]
5. Wong, W.; Wong, H.Y.; Badruzzaman, A.B.M.; Goh, H.H.; Zaman, M. Recent advances in exploitation of nanomaterial for arsenic removal from water: A review. *Nanotechnology* **2017**, *28*, 042001. [[CrossRef](#)] [[PubMed](#)]
6. Ahmed, N.; Haider, W. Heterogeneous photocatalysis and its potential applications in water and wastewater treatment: A review. *Nanotechnology* **2018**, *29*, 342001. [[CrossRef](#)] [[PubMed](#)]
7. McLaren, A.; Valdes-Solis, T.; Li, G.; Tsang, S.C. Shape and size effects of ZnO nanocrystals on photocatalytic activity. *J. Am. Chem. Soc.* **2009**, *131*, 12540–12541. [[CrossRef](#)]
8. Xu, T.; Zhang, L.; Cheng, H.; Zhu, Y. Significantly enhanced photocatalytic performance of ZnO via graphene hybridization and the mechanism study. *Appl. Catal. B Environ.* **2011**, *101*, 382–387. [[CrossRef](#)]
9. Gröttrup, J.; Schütt, F.; Smazna, D.; Lupan, O.; Adelung, R.; Mishra, Y.K. Porous ceramics based on hybrid inorganic tetrapodal networks for efficient photocatalysis and water purification. *Ceram. Int.* **2017**, *43*, 14915–14922. [[CrossRef](#)]
10. Ahmed, G.; Hanif, M.; Zhao, L.; Hussain, M.; Khan, J.; Liu, Z. Journal of Molecular Catalysis A: Chemical Defect engineering of ZnO nanoparticles by graphene oxide leading to enhanced visible light photocatalysis. *J. Mol. Catal. A Chem.* **2016**, *425*, 310–321. [[CrossRef](#)]
11. Low, J.; Yu, J.; Jaroniec, M.; Wageh, S.; Al-Ghamdi, A.A. Heterojunction Photocatalysts. *Adv. Mater.* **2017**, *29*, 1601694. [[CrossRef](#)]
12. Lv, T.; Pan, L.; Liu, X.; Sun, Z. Enhanced photocatalytic degradation of methylene blue by ZnO-reduced graphene oxide-carbon nanotube composites synthesized via microwave-assisted reaction. *Catal. Sci. Technol.* **2012**, *2*, 2297–2301. [[CrossRef](#)]
13. Rokhsat, E.; Akhavan, O. Improving the photocatalytic activity of graphene oxide/ZnO nanorod films by UV irradiation. *Appl. Surf. Sci.* **2016**, *371*, 592–595. [[CrossRef](#)]
14. She, P.; Yin, S.; He, Q.; Zhang, X.; Xu, K.; Shang, Y.; Men, X.; Zeng, S.; Sun, H.; Liu, Z. A self-standing macroporous Au/ZnO/reduced graphene oxide foam for recyclable photocatalysis and photocurrent generation. *Electrochim. Acta* **2017**, *246*, 35–42. [[CrossRef](#)]
15. Bai, X.; Sun, C.; Liu, D.; Luo, X.; Li, D.; Wang, J.; Wang, N.; Chang, X.; Zong, R.; Zhu, Y. Photocatalytic degradation of deoxyvalenol using graphene/ZnO hybrids in aqueous suspension. *Appl. Catal. B Environ.* **2017**, *204*, 11–20. [[CrossRef](#)]

16. Khalil, A.; Gondal, M.A.; Dastageer, M.A. Augmented photocatalytic activity of palladium incorporated ZnO nanoparticles in the disinfection of Escherichia coli microorganism from water. *Appl. Catal. A Gen.* **2011**, *402*, 162–167. [[CrossRef](#)]
17. Adhikari, S.; Gupta, R.; Surin, A.; Kumar, T.S.; Chakraborty, S.; Sarkar, D.; Madras, G. Visible light assisted improved photocatalytic activity of combustion synthesized spongy-ZnO towards dye degradation and bacterial inactivation. *RSC Adv.* **2016**, *6*, 80086–80098. [[CrossRef](#)]
18. Liu, X.; Pan, L.; Lv, T.; Lu, T.; Zhu, G.; Sun, Z.; Sun, C. Microwave-assisted synthesis of ZnO-graphene composite for photocatalytic reduction of Cr(vi). *Catal. Sci. Technol.* **2011**, *1*, 1189–1193. [[CrossRef](#)]
19. Singh, S.; Barick, K.C.; Bahadur, D. Fe<sub>3</sub>O<sub>4</sub> embedded ZnO nanocomposites for the removal of toxic metal ions, organic dyes and bacterial pathogens. *J. Mater. Chem. A* **2013**, *1*, 3325. [[CrossRef](#)]
20. Chong, M.N.; Jin, B.; Chow, C.W.K.; Saint, C. Recent developments in photocatalytic water treatment technology: A review. *Water Res.* **2010**, *44*, 2997–3027. [[CrossRef](#)]
21. Giovannetti, G.; Khomyakov, P.A.; Brocks, G.; Karpan, V.M.; van den Brink, J.; Kelly, P.J. Doping graphene with metal contacts. *Phys. Rev. Lett.* **2008**, *101*, 4–7. [[CrossRef](#)]
22. Roy, P.; Periasamy, A.P.; Liang, C.T.; Chang, H.T. Synthesis of graphene-ZnO-Au nanocomposites for efficient photocatalytic reduction of nitrobenzene. *Environ. Sci. Technol.* **2013**, *47*, 6688–6695. [[CrossRef](#)] [[PubMed](#)]
23. Malato, S.; Fernandez-Ibanez, P.; Maldonado, M.I.; Blanco, J.; Gernjak, W. Decontamination and disinfection of water by solar photocatalysis: Recent overview and trends. *Catal. Today* **2009**, *147*, 1–59. [[CrossRef](#)]
24. Xu, S.; Fu, L.; Pham, T.S.; Yu, A.; Han, F.; Chen, L. Preparation of ZnO flower/reduced graphene oxide composite with enhanced photocatalytic performance under sunlight. *Ceram. Int.* **2015**, *41*, 4007–4013. [[CrossRef](#)]
25. Xue, B.; Zou, Y. High photocatalytic activity of ZnO—Graphene composite. *J. Colloid Interface Sci.* **2018**, *529*, 306–313. [[CrossRef](#)] [[PubMed](#)]
26. Luan, V.H.; Tien, H.N.; Hur, S.H. Fabrication of 3D structured ZnO nanorod/reduced graphene oxide hydrogels and their use for photo-enhanced organic dye removal. *J. Colloid Interface Sci.* **2015**, *437*, 181–186. [[CrossRef](#)] [[PubMed](#)]
27. Marcano, D.C.; Kosynkin, D.V.; Berlin, J.M.; Sinitskii, A.; Sun, Z.; Slesarev, A.; Alemany, L.B.; Lu, W.; Tour, J.M. Improved Synthesis of Graphene Oxide. *ACS Nano* **2010**, *4*, 4806–4814. [[CrossRef](#)]